

# Power Correlations and Mixing Patterns of Several Large Paddle Impellers with Dished Bottoms

Haruki FURUKAWA, Yoshihito KATO, Tomoho KATO and Yutaka TADA  
Department of Life and Materials Engineering, Nagoya Institute of Technology,  
Gokiso-cho, Showa -ku, Nagoya-shi, Aichi 466-8555, Japan

**Keywords:** Mixing, Agitation, Power Number, Large Paddle Impeller, Mixing Pattern

Power numbers of several large two-blade paddle impellers in stirred vessels with dished bottoms were measured for a wide range of Reynolds numbers. Mixing patterns of these impellers with dished bottoms were observed for a wide range of Reynolds numbers by using a decolorization method based on the reaction between sodium thiosulfate and iodine. The power numbers of these impellers can be correlated with the modified correlation of Kamei et al. A relationship was established between the power number diagram ( $N_p$ - $Re$  diagram) and the shape of the isolated zone. At low Reynolds numbers, complicated isolated zones were observed, while a cylindrically rotating isolated zone was not observed.

## Introduction

Mixing is one of the most important unit operations in chemical and biochemical industries. For the accurate design and operation of a stirred vessel, it is necessary to plot the power number against the Reynolds number. In an unbaffled vessel, the power number  $N_p$  ( $P/(\rho n^3 d^5)$ ) is inversely proportional to the Reynolds number  $Re$  ( $nd^2\rho/\mu$ ) for laminar mixing, while for turbulent mixing,  $N_p$  decreases gradually with an increase in  $Re$ . When a baffled vessel is used,  $N_p$  is inversely proportional to  $Re$  during laminar mixing, which is also the case in an unbaffled vessel. During turbulent mixing in a baffled vessel,  $N_p$  is constant regardless of the baffle conditions, but it increases with the number of baffles. The power number diagram is typical to a given impeller/mixing vessel combination.

It is well known that in an unbaffled vessel, an isolated zone (a doughnut-ring-shaped zone during laminar mixing and a cylindrically rotating zone (CRZ) during turbulent mixing) may be generated when using relatively small impellers such as propeller impellers and turbine impellers (Kato *et al.*, 2010). However, the value of  $Re$  when the doughnut-ring-shaped isolated zone becomes a CRZ has not been determined. Mixing is inefficient in the isolated zone. However, it is known that several large paddle impellers developed by mixer companies in Japan can be useful over a wide range of Reynolds number.

Kato *et al.* (2012) measured the power consumptions of several wide paddle impellers over a wide range of Reynolds number, from laminar to turbulent flow regions, and correlated them by using modified versions of Kamei (Kamei *et al.*, 1995, 1996) and Hiraoka's (Hiraoka *et al.*, 1997) expressions. However, this expression cannot well correlate the use of the mixing vessel with a dished

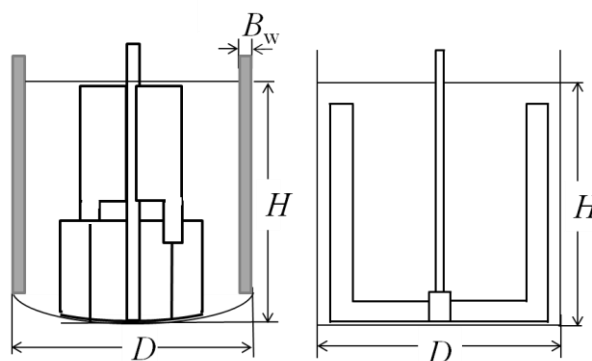


**Fig. 1** Example of schematic diagram of mixing vessels with dished (left) and flat (right) bottoms

bottom.

In this paper, we propose the new power correlations of impellers with dished bottoms and derive a relationship between the power number diagram and the shape of the mixing pattern.

## 1. Experimental

A schematic diagram of the stirred vessels used in this study is shown in **Figure 1**. The vessel, which was used for the measuring power consumption and observing mixing patterns, was cylindrical vessel and had an inner diameter ( $D$ ) of 185 mm. The vessel incorporated two baffles on the sidewall,  $B_w = D/10$ . MAXBLEND (Sumitomo Heavy Industries Process Equipment Co. Ltd.), FULLZONE (Kobelco eco-solutions Co.Ltd.), Supermix impellers (Satake Chemical Equipment Mfg. Ltd.) and an anchor impeller are used as the large two-blade paddles, which are given in **Figure 2**. The geometry of the impellers are shown in **Table 1**. The impellers were set near the vessel bottom as shown in Figure 1. The liquids used for measuring the power consumption and observing the mixing patterns

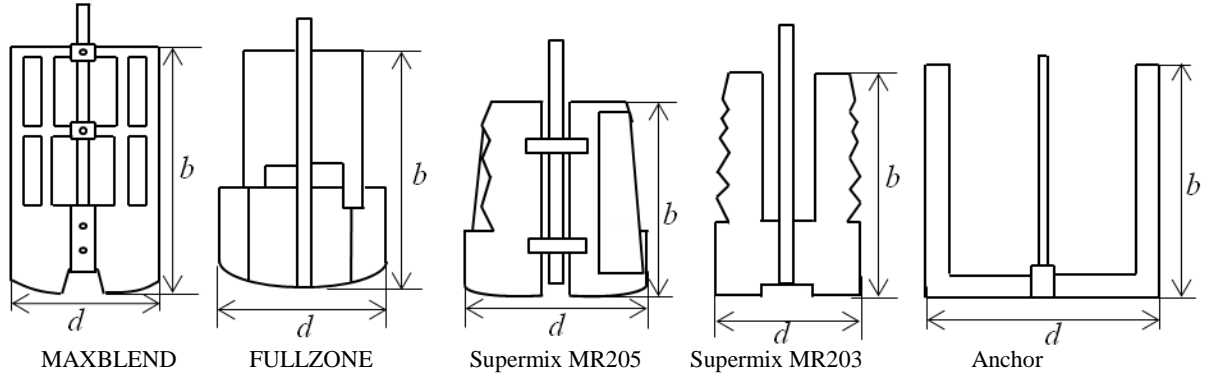


**Fig.2** Large paddle impellers. Values of  $b$  and  $d$  are listed in Table 1

were desalted water and starch syrup solution ( $\mu = 0.001 - 2.5$  Pas). The vessel was filled to a height equal to the vessel diameter ( $H = D$ ). The power consumption  $P$  ( $=2\pi nT$ ) was calculated by measuring the shaft torque  $T$  and rotational speed  $n$ . The mixing pattern was observed by adopting the decolorization method based on the reaction of iodine with sodium thiosulfate in water.  $n$  was varied from 30 to 100 rpm. The mixing vessel was immersed in a rectangular water-filled chamber in order to minimize optical distortions caused by the curvature of the tank. To achieve homogeneous illumination, a sheet of white paper on the rectangular chamber wall was used as a light diffuser. Sodium thiosulfate was added between the bottom paddle and the vessel wall. The mixing pattern was observed and recorded by a CCD camera for 60 min..

**Table 1** Geometry of large paddle impellers

Impeller	$d$ [m]	$b$ [m]
MAXBLEND	0.119	0.180
FULLZONE	0.113	0.186
Supermix MR203	0.104	0.160
MR205	0.132	0.150
Anchor	0.165	0.165

**Table 2** Correlation of Kato *et al.*, (2012) for large paddle impellers with flat bottom (except Anchor impeller)

**Unbaffled condition**

$$N_{P0} = \{[1.2\pi^4\beta^2]/[8d^3/(D^2H)]\}f$$

$$f = C_L/Re_G + C_t\{[(C_{tr}/Re_G) + Re_G]^{-1} + (f_{\infty}/C_t)^{1/m}\}^m$$

$$Re_d = nd^2\rho/\mu, \quad Re_G = \{[\pi\eta\ln(D/d)]/(4d/\beta D)\}Re_d$$

$$C_L = 0.215\eta n_p(d/H)[1-(d/D)^2] + 1.83(b/H)(n_p/2)^{1/3}$$

$$C_t = [(1.1X^{2.5})^{-7.8} + (0.25)^{-7.8}]^{-1/7.8}$$

$$m = [(0.71X^{0.373})^{-7.8} + (0.333)^{-7.8}]^{-1/7.8}$$

$$C_{tr} = 1000(d/D)^{-3.24}(b/D)^{-1.18}X^{-0.74}$$

$$f_{\infty} = 0.0151(d/D)C_t^{0.308}$$

$$X = \eta n_p^{0.7}b/H$$

$$\beta = 2\ln(D/d)/[(D/d)-(d/D)]$$

$$\gamma = [\eta\ln(D/d)/(\beta D/d)^5]^{1/3}$$

$$\eta = 0.711\{0.157 + [n_p \ln(D/d)]^{0.611}\} / \{n_p^{0.52}[1-(d/D)^2]\}$$

**Baffled condition**

$$N_p = [(1+x^{-3})^{-1/3}]N_{Pmax}$$

$$x = 3.0(B_w/D)n_B^{0.8}/N_{Pmax}^{0.2} + N_{P0}/N_{Pmax}$$

**Fully baffled condition**

$$N_{Pmax} = 5.0(b/d)^{0.75}$$

**2. Results and Discussion**

**2.1 Power correlations**

The power number  $N_p$  value of MAXBLEND with a dished bottom was well correlated with the equations shown in **Table 3**, as given in **Figure 3**.  $N_p$  values of FULLZONE and Supermix MR205 with dished bottoms were well correlated with the equations given in **Table 4**, as shown in **Figure 4**.  $C_t$  and  $m$  in the tables are modified for these impellers with dished bottoms. For Supermix MR203, the correlation given in **Table 2** can be used for a vessel with a flat bottom.

**Table 3** New Correlation of MAXBLEND with dished bottom

**Unbaffled condition**

$$N_{P0} = \{[1.2\pi^4\beta^2]/[8d^3/(D^2H)]\}f$$

$$f = C_L/Re_G + C_t\{[(C_{tr}/Re_G) + Re_G]^{-1} + (f_{\infty}/C_t)^{1/m}\}^m$$

$$Re_d = nd^2\rho/\mu, \quad Re_G = \{[\pi\eta\ln(D/d)]/(4d/\beta D)\}Re_d$$

$$C_L = 0.215\eta n_p(d/H)[1-(d/D)^2] + 1.83(b/H)(n_p/2)^{1/3}$$

$$C_t = [(0.47X^{2.5})^{-7.8} + (0.25)^{-7.8}]^{-1/7.8}$$

$$m = [(0.71X^{0.373})^{-7.8} + (0.333)^{-7.8}]^{-1/7.8}$$

$$C_{tr} = 1000(d/D)^{-3.24}(b/D)^{-1.18}X^{-0.74}$$

$$f_{\infty} = 0.0151(d/D)C_t^{0.308}$$

$$X = \eta n_p^{0.7}b/H$$

$$\beta = 2\ln(D/d)/[(D/d)-(d/D)]$$

$$\gamma = [\eta\ln(D/d)/(\beta D/d)^5]^{1/3}$$

$$\eta = 0.711\{0.157 + [n_p \ln(D/d)]^{0.611}\} / \{n_p^{0.52}[1-(d/D)^2]\}$$

**Baffled condition**

$$N_p = [(1+x^{-3})^{-1/3}]N_{Pmax}$$

$$x = 3.0(B_w/D)n_B^{0.8}/N_{Pmax}^{0.2} + N_{P0}/N_{Pmax}$$

### Fully baffled condition

$$N_{Pmax} = 5.0(b/d)^{0.75}$$

**Table 4** New Correlation of FULLZONE with dished bottom

### Unbaffled condition

$$N_{P0} = \{[1.2\pi^2\beta^2]/[8d^3/(D^2H)]\}f$$

$$f = C_L/Re_G + C_i\{[(C_r/Re_G) + Re_G]^{-1} + (f_{\infty}/C_i)^{1/m}\}^m$$

$$Re_d = nd^2\rho/\mu, \quad Re_G = \{[\pi\eta\ln(D/d)]/(4d/\beta D)\}Re_d$$

$$C_L = 0.215\eta_p(d/H)[1-(d/D)^2] + 1.83(b/H)(n_p/2)^{1/3}$$

$$C_i = [(0.28X^{2.5})^{-7.8} + (0.25)^{-7.8}]^{-1/7.8}$$

$$m = [(0.71X^{0.373})^{-7.8} + (0.333)^{-7.8}]^{-1/7.8}$$

$$C_r = 3000(d/D)^{-3.24}(b/D)^{-1.18}X^{-0.74}$$

$$f_{\infty} = 0.0151(d/D)C_i^{0.308}$$

$$X = \eta_p^{0.7}b/H$$

$$\beta = 2\ln(D/d)/[(D/d)-(d/D)]$$

$$\gamma = [\eta\ln(D/d)/(\beta D/d)^5]^{1/3}$$

$$\eta = 0.711\{0.157 + [n_p \ln(D/d)]^{0.611}\} / \{n_p^{0.52}[1-(d/D)^2]\}$$

### Baffled condition

$$N_P = [(1+x^{-3})^{-1/3}]N_{Pmax}$$

$$x = 3.0(B_w/D)n_B^{0.8}/N_{Pmax}^{0.2} + N_{P0}/N_{Pmax}$$

### Fully baffled condition

$$N_{Pmax} = 5.0(b/d)^{0.75}$$

## 2.2 Mixing Patterns

### 2.2.1 MAXBLEND

The power consumptions and  $Re$  determined while observing the mixing patterns in the baffled ( $n_b = 2$ ,  $B_w/D = 0.1$ ) and unbaffled vessels with MAXBLEND are shown in **Figure 5**. **Figures 6** and **7** show the characteristic mixing patterns in the unbaffled and baffled vessels, respectively. These photographs were taken at nondimensional agitation time  $nt = 200$  when typical mixing patterns were generated. At a low  $Re = 6 - 10$ , a poorly-mixed zone could be observed near the bottom paddle, regardless of whether the baffle present or not. However, the poorly mixed zone was dissipated by long time mixing.

At  $Re = 40$  in the unbaffled vessel, which is in Figure 5 the point at which curves for the baffled and unbaffled vessels depart from each other, a thin doughnut ring was observed, while in the baffled vessel two small poorly-mixed zones rotated with the impeller near the vessel bottom, as shown in Figure 17 in detail. For  $Re > 80$ , a poorly-mixed zone was not observed, regardless of whether the baffle was present or not.

### 2.2.2 FULLZONE

The power consumptions and  $Re$  determined while observing the mixing patterns in the baffled ( $n_b = 2$ ,  $B_w/D = 0.1$ ) and unbaffled vessels with FULLZONE are shown in **Figure 8**. **Figures 9** and **10** show the

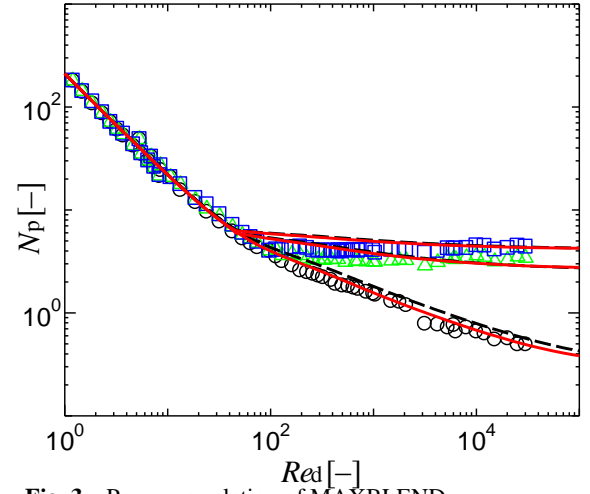


**Fig. 3** Power correlation of MAXBLEND

○: observed without baffle, △: observed with two baffles, □: observed with four baffles, black broken line: correlation line of Table 2, red solid line: correlation of this work of Table 3

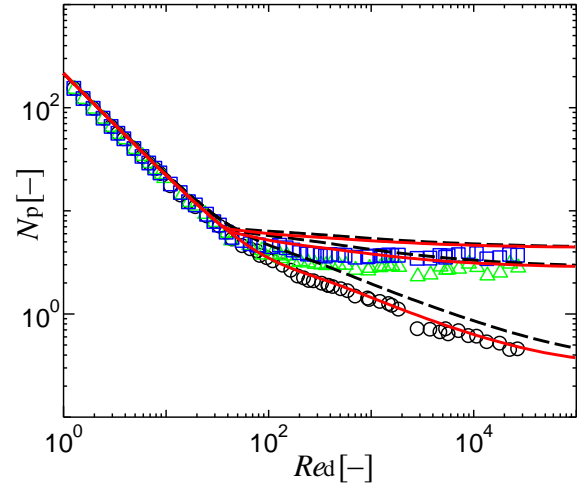


**Fig. 4** Power correlation of FULLZONE

The symbols and lines are the same as in Figure 3. black broken line: correlation line of Table 2, red solid line: correlation of this work of Table 4

characteristic mixing patterns in the unbaffled and baffled vessels, respectively. These photographs were taken at nondimensional agitation time  $nt = 200$ . At a low  $Re = 6 - 15$ , poorly-mixed zone can be observed at the vessel top, regardless of whether the baffle was present or not.

At  $Re = 40$  in the unbaffled vessel, which is the point in Figure 8 at which curves for the baffled and unbaffled vessels, a thin doughnut ring was observed, whereas in the baffled vessel at  $Re = 80$  two small poorly mixed zones like ring rotated with impeller near vessel bottom, which is shown in Figure 17 in detail. For  $Re > 80$ , poorly mixed zone was not observed, regardless of whether the baffle was present or not. However the poorly-mixed zone can be dissipated by long time mixing.

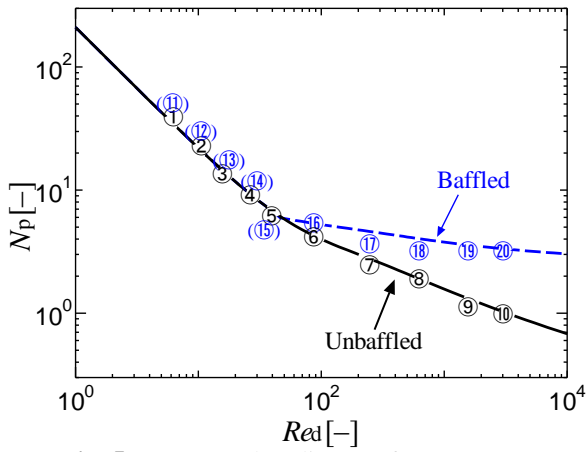


**Fig. 5** Power number diagram for MAXBLEND

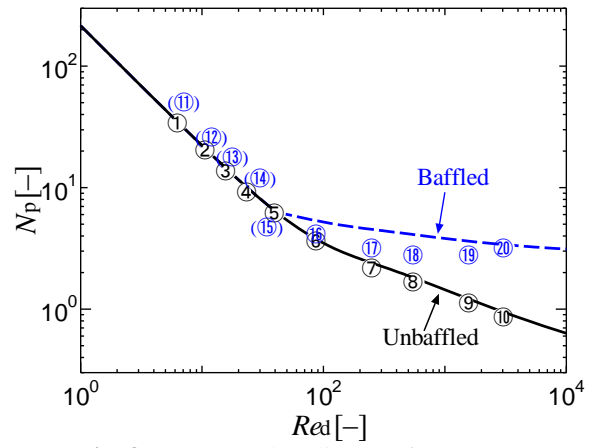


**Fig. 8** Power number diagram for FULZONE

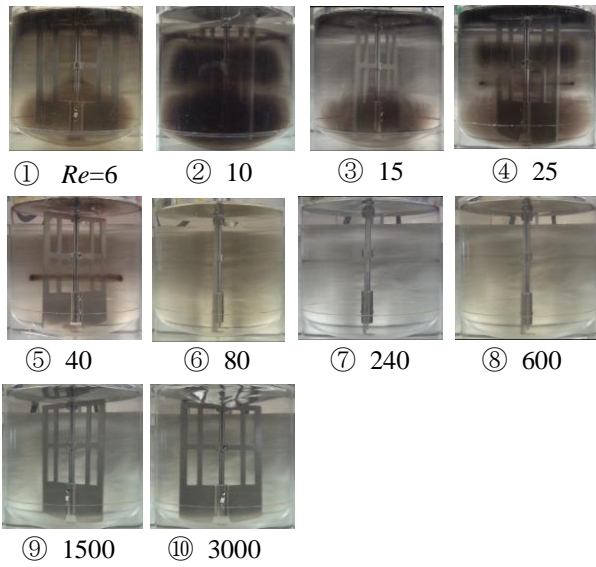


**Fig. 6** Mixing patterns obtained with MAXBLEND in an unbaffled vessel

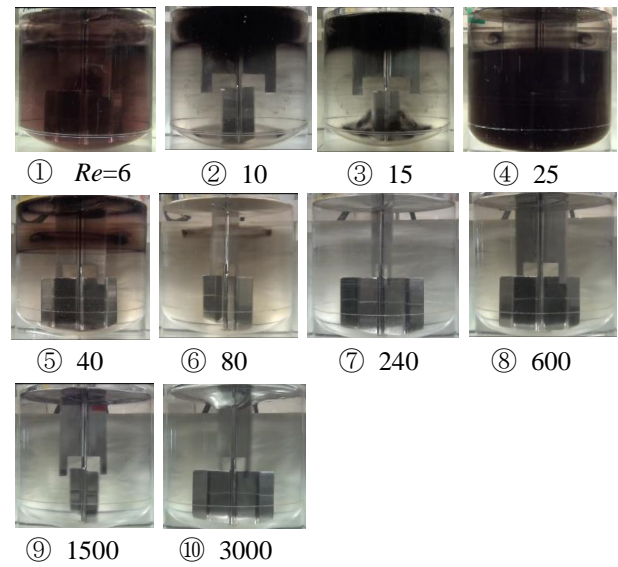


**Fig. 9** Mixing patterns obtained with FULZONE in an unbaffled vessel

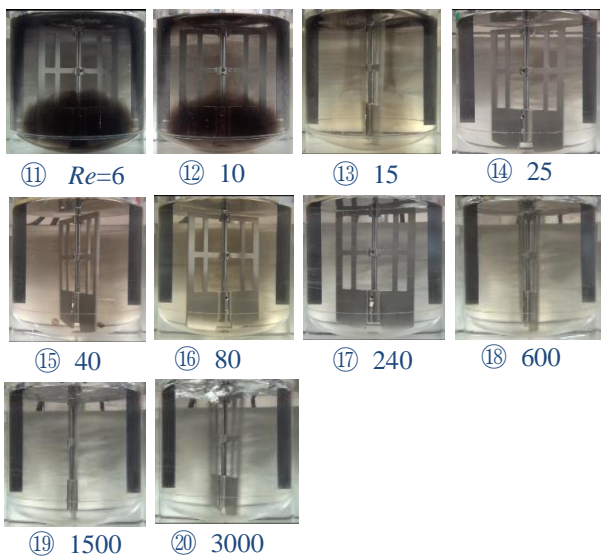


**Fig. 7** Mixing patterns obtained with MAXBLEND in a baffled vessel

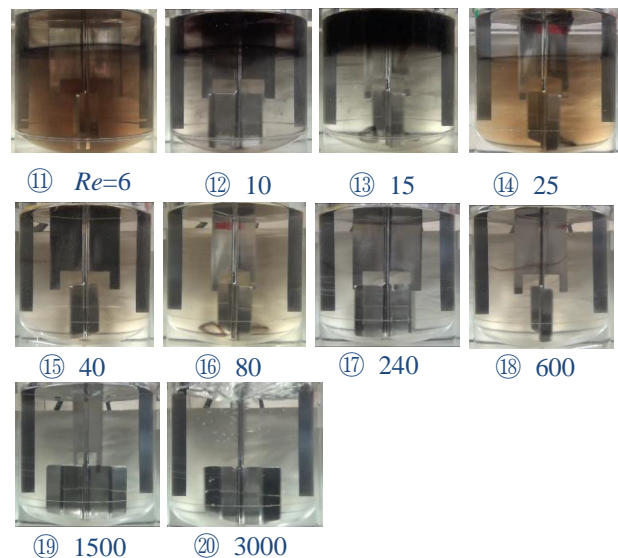


**Fig. 10** Mixing patterns obtained with FULZONE in a baffled vessel

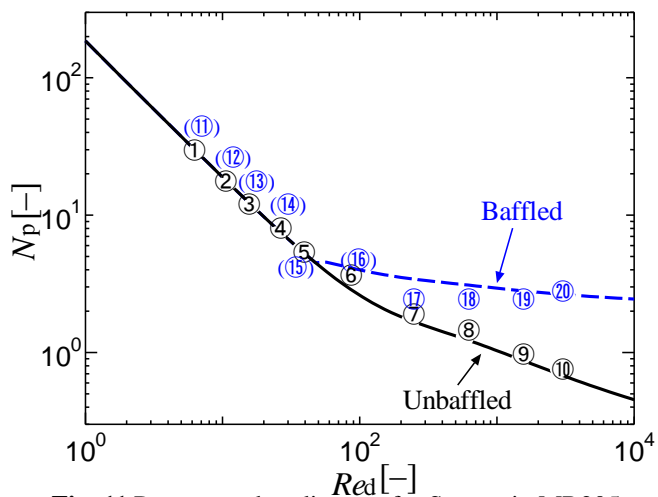


**Fig. 11** Power number diagram for Supermix MR205

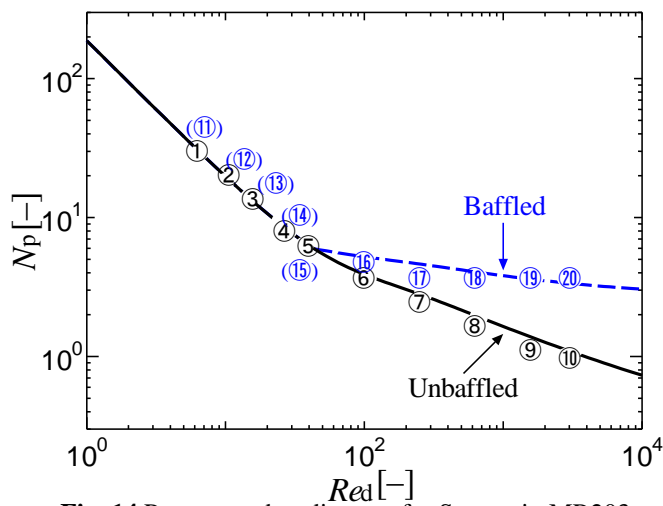


**Fig. 14** Power number diagram for Supermix MR203

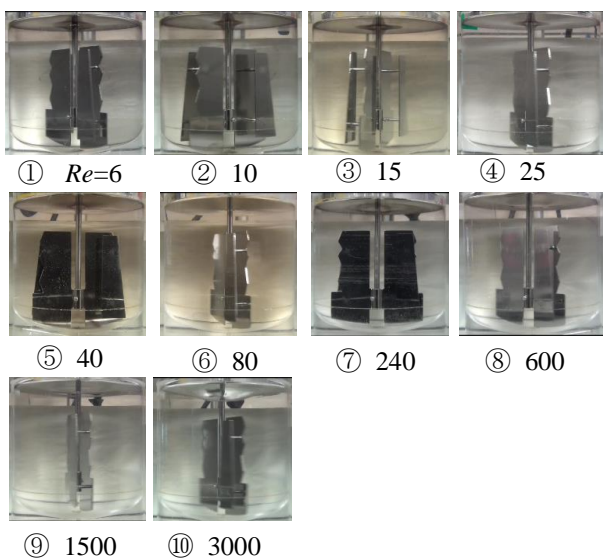


**Fig. 12** Mixing patterns obtained with Supermix MR205 in un baffled vessel

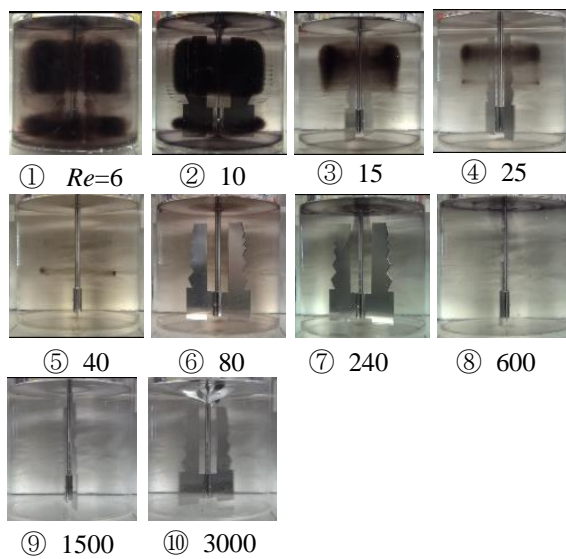


**Fig. 15** Mixing patterns obtained with Supermix MR203 in un baffled vessel

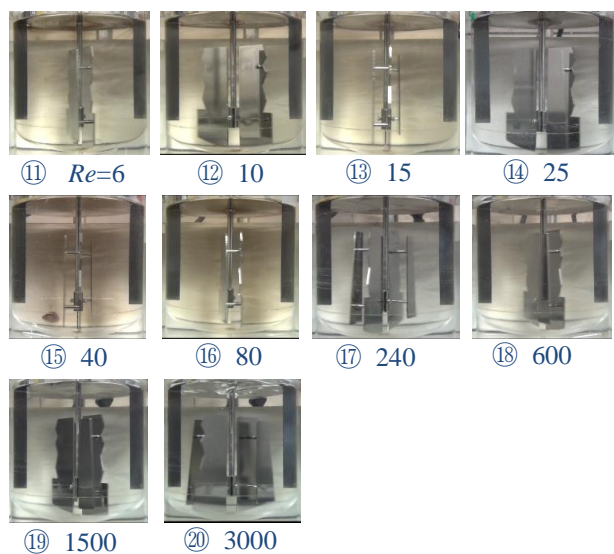


**Fig. 13** Mixing patterns obtained with Supermix MR205 in baffled vessel

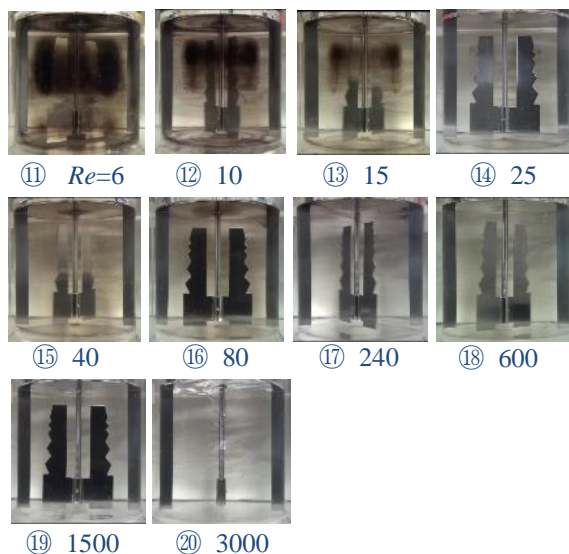


**Fig. 16** Mixing patterns obtained with Supermix MR203 in baffled vessel

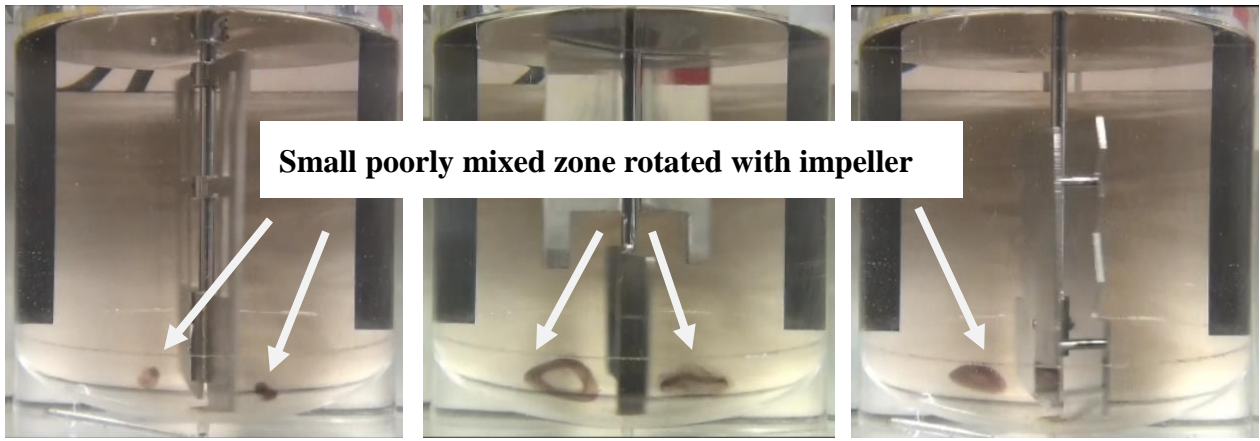


**Fig. 17** Small poorly mixed zone rotated with large impellers, except MR203, in baffled vessel at  $Re = 40$

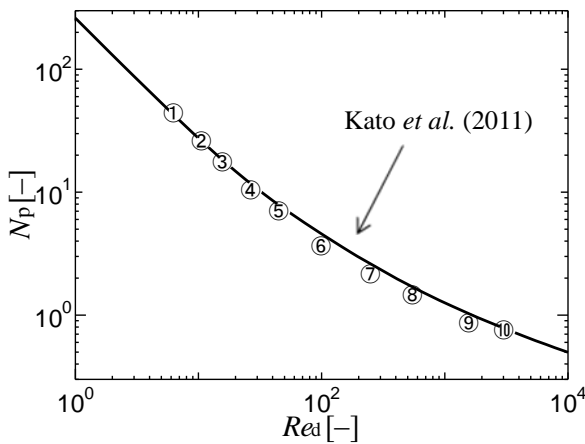


**Fig. 18** Power number diagram for anchor impeller

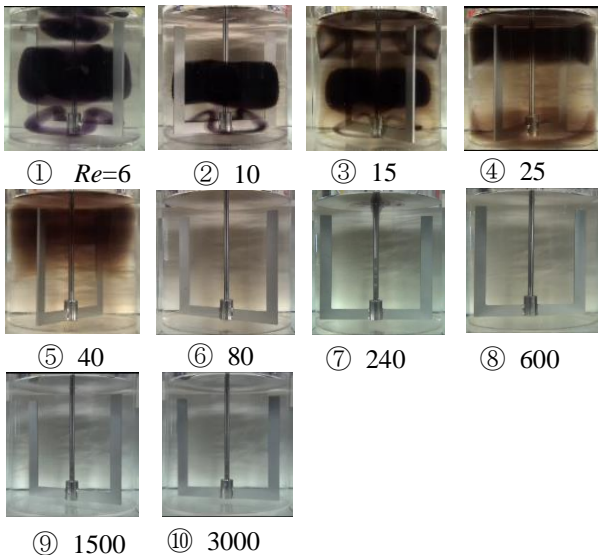


**Fig. 19** Mixing patterns obtained with an Anchor in an unbaffled vessel

### 2.2.3 Supermix MR205

The power consumptions and  $Re$  determined while observing the mixing patterns in the baffled ( $n_b = 2$ ,  $B_w/D = 0.1$ ) and unbaffled vessels with Supermix MR205 are shown in **Figure 11**. **Figures 12 and 13** show the characteristic mixing patterns in the unbaffled and

baffled vessels, respectively. These photographs were taken at nondimensional agitation time  $nt = 200$ . A poorly mixed zone could not be observed, regardless of whether the baffle was present or not. However, only one small poorly mixed zone was observed at  $Re = 40$  in the baffled vessel (as noted in **Figure 17**).

### 2.2.4 Supermix MR203

The power consumptions and  $Re$  determined while observing the mixing patterns in the baffled ( $n_b = 2$ ,  $B_w/D = 0.1$ ) and unbaffled vessels with Supermix MR203 are shown in **Figure 14**. **Figures 15 and 16** show the characteristic mixing patterns in the unbaffled and baffled vessels, respectively. These photographs were taken at nondimensional agitation time  $nt = 200$ . At low Reynolds number, large poorly mixed zones were observed, regardless of whether the baffle was present or not. It was considered that an auxiliary impeller was very important for mixing operation, as MR203 does not have an auxiliary impeller. **Figure 17** shows small poorly mixed zone like ring rotated with a large impeller, except MR203 near the vessel bottom. Such a zone was not observed in the vessel with MR203.

### 2.2.5 Anchor

**Figures 18 and 19** show the power diagram and the characteristic mixing patterns for anchor impeller. These photographs were recorded at non dimensional agitation time  $nt = 1000$  (not 200). Even for  $Re > 40$ , multiple large poorly mixed zones were observed, regardless of whether the baffle was present or not. It was considered that the anchor impeller was inconvenient for liquid mixing.

## Conclusions

From the photographs of the mixing patterns observed in this study, we could determine three regions in the power number diagram. When  $Re$  is less than 10, the

power number is inversely proportional to  $Re$ , the poorly mixed zone was generated. However, in the turbulent region, a CRZ was not generated for an unbaffled vessel. The mixing pattern observed with any impeller, including the traditional paddle, pitched paddle, and propeller impeller, can be predicted from the power correlation.

#### Nomenclature

$B_w$	= baffle width	[m]
$b$	= height of impeller blade	[m]
$C$	= clearance between vessel bottom and impeller	[m]
$D$	= vessel diameter	[m]
$d$	= impeller diameter	[m]
$H$	= liquid depth	[m]
$m$	= correlation parameter	[-]
$N_p$	= power number ( $P/\rho n^3 d^5$ )	[-]
$N_{p0}$	= power number under unbaffled conditions	[-]
$N_{pmax}$	= power number under fully baffled conditions	[-]
$n$	= impeller rotational speed	[-]
$n_b$	= number of baffle plates	[-]
$n_p$	= number of impeller blades	[-]
$P$	= power consumption	[W]
$Re$	= impeller Reynolds number ( $nd^2\rho/\mu$ )	[-]
$T$	= shaft torque	[Nm]
$t$	= agitation time	[s <sup>-1</sup> ]
$\mu$	= liquid viscosity	[Pas]
$\rho$	= liquid density	[kg/m <sup>3</sup> ]

#### Literature Cited

- Hiraoka, S., N. Kamei, Y. Kato, Y. Tada, H.G. Chun and T. Yamaguchi; “Power Correlation for Pitched Blade Paddle Impeller in Agitated Vessels with and without Baffles,” *Kagaku Kogaku Ronbunshu*, **23**, 969–975 (1997)
- Kamei, N., S. Hiraoka, Y. Kato, Y. Tada, H. Shida, Y. S. Lee, T. Yamaguchi and S.T. Koh; “Power Correlation for Paddle Impellers in Spherical and Cylindrical Agitated Vessels,” *Kagaku Kogaku Ronbunshu*, **21**, 41–48 (1995)
- Kamei, N., S. Hiraoka, Y. Kato, Y. Tada, K. Iwata, K. Murai, Y. S. Lee, T. Yamaguchi and S. T. Koh; “Effects of Impeller and Baffle Dimensions on Power Consumption under Turbulent Flow in an Agitated Vessel with Paddle Impeller,” *Kagaku Kogaku Ronbunshu*, **22**, 249–256 (1996)
- Kato Y., Y. Tada, Y. Takeda, N. Atsumi and Y. Nagatsui; “Prediction of Mixing Pattern from Power Number Diagram in Baffled and Unbaffled Mixing Vessels,” *J. Chem. Eng. Japan*, **43**, 46–51 (2010)
- Kato, Y., N. Kamei, Y. Tada, N. Kato, T. Kato, T. Ibuki, H. Furukawa and Y. Nagatsu; “Power Consumption of Anchor Impeller over Wide Range of Reynolds Number,” *Kagaku Kogaku Ronbunshu*, **37**, 19–21 (2011)
- Kato, Y., A. Obata, T. Kato, H. Furukawa and Y. Tada; “Power